Gas phase photocatalytic spiral reactor for fast and efficient pollutant degradation

Gas phase photocatalytic spiral reactor for fast and efficient pollutant degradation

Natan Blommaerts,[1] Ramesh Asapu,[1] Nathalie Claes,[2] Sara Bals,[2] Silvia Lenaerts,[1] Sammy W. Verbruggen[1,3,*]

[1] Sustainable Energy, Air & Water Technology (DuEL), Department of Bioscience Engineering, University of Antwerp, Groenenborgerlaan 171, 2020 Antwerp, Belgium

[2] EMAT, Department of Physics, University of Antwerp, Groenenborgerlaan 171, 2020 Antwerp, Belgium

[3] Center for Surface Chemistry and Catalysis (COK), Department of Microbial and Molecular Systems, KU Leuven, Celestijnenlaan 200F, 3001 Heverlee, Belgium

* Sammy.Verbruggen@uantwerp.be

Abstract

Photocatalytic reactors for the degradation of gaseous organic pollutants often suffer from major limitations such as small reaction area, sub-optimal irradiation conditions and thus limited reaction rate. In this work, an alternative solution is presented that involves a glass tube coated on the inside with (silver-modified) TiO_2 and spiraled around a UVA lamp. First, the spiral reactor is coated from the inside with TiO_2 using an experimentally verified procedure that is optimized toward UV light transmission. This procedure is kept as simple as possible and involves a single casting step of a 1 wt% suspension of TiO_2 in ethanol through the spiral. This results in a coated tube that absorbs nearly all incident UV light under the experimental conditions used. The optimized coated spiral reactor is then benchmarked to a conventional annular photoreactor of the same outer dimensions and total catalyst loading over a broad range of experimental conditions. Although residence time distribution experiments indicate slightly longer dwelling of molecules in the spiral reactor, no significant difference in by-passing of gas between the spiral reactor and the annular reactor can be claimed. Acetaldehyde degradation efficiency of 100% is obtained with the spiral reactor for a residence time as low as 60 s, whereas the annular reactor could not achieve full degradation even at 1000 s residence time. In a final case study, addition of long-term stable silver nanoparticles, protected by an ultra-thin polymer shell applied via the layer-by-layer (LbL) method, to the spiral

reactor coating is shown to double the degradation efficiency and provides an interesting strategy to cope with higher pollutant concentrations without changing the overall dimensions.

Keywords

Photocatalysis, titanium dioxide (TiO_2), spiral, acetaldehyde, silver, plasmon, VOC, gas phase

1 Introduction

Photocatalysis is a promising technology for pollution abatement in aqueous and gaseous environment, especially degradation of volatile organic compounds (VOC).[1,2] The photocatalytic process is based on light-induced generation of electron-hole pairs that initiate oxidation and reduction reactions of pollutants on the catalyst surface. Typically, photocatalytic reactors for air purification are based on the immobilization of the catalyst onto a surface.[3] An ideal photoreactor for air purification should have (1) an appropriate light source irradiating the catalyst surface, (2) the catalyst coating should have a large surface area to ensure availability of many active sites, (3) high mass transfer and (4) low pressure drop.[4] The most widely used gas phase photocatalytic reactors are the flat plate reactor and the annular reactor. The flat plate reactor is one of the most straightforward geometries and consists of a coated flat substrate that is illuminated from the top by UV lamps.[5–9] The airflow runs parallel to the flat plate. Advantages of this type of reactor are simplicity and small pressure drop. A significant disadvantage is that only a small reaction area can be achieved. The annular type reactor is built up from two concentric cylinders resulting in an annular gap.[10–15] The catalyst is coated on the interior wall(s) of the cylinder(s) and the light source is usually positioned longitudinally in the center of the reactor. Also for this geometry the small reaction area remains an important disadvantage. More complex reactor types have also been developed and include for example a monolith reactor.[16] This reactor contains a certain number of channels and provides a large catalyst surface area and a low pressure drop. The major drawback of this type is the top irradiation that is insufficient, and results in a limited reaction rate.[17]

The goal of this work is to overcome the aforementioned shortcomings by developing and optimizing an unconventional reactor design based on a glass spiral surrounding the light source, for the efficient photocatalytic degradation of acetaldehyde. Such a spiraled reactor configuration has already proven to be quite beneficial in various research areas, such as water treatment,[18–20] non-catalyzed microfluidic photochemical transformations, and it even enables efficient photo-inactivation of a Herpes virus strain and rapid photo-destruction of dyes and pharmaceuticals in aqueous streams.[21]

In this work we investigate the use of a spiral reactor for gas phase photocatalytic applications, by coating the entire interior of the spiral tube with TiO_2 using a fast and convenient coating procedure,[6,22] so that the catalyst coverage is optimized with respect to the amount of light transmission. This is a first significant improvement of the work by Araña *et al.*, who provided convincing evidence of the usefulness of a spiral reactor for the degradation of gaseous compounds.[23] In addition, we provide an insightful benchmark of the optimized gas phase spiral reactor against a conventional annular reactor with the same outer dimensions and catalyst loading by evaluating the degradation efficiency of acetaldehyde over a wide range of reaction conditions. Acetaldehyde is an important compound both in indoor and outdoor environments and is an underestimated risk factor for cancer development.[24–26] In summary, the advantages of this spiral reactor are (1) a very homogeneous light distribution over the entire reactor, (2) Intense contact between pollutants and the catalyst surface and (3) a large reaction area, (4) leading to high pollutant degradation efficiency, (5) all in a very compact design.

To further increase the light efficiency and hence the photocatalytic degradation efficiency, silver nanoparticles are deposited onto the TiO_2 surface. When irradiated with light of the correct wavelength, noble metal nanoparticles display surface plasmon resonance (SPR), *i.e.* the coherent oscillation of the negative electron cloud against the restoring force of the positive nucleus.[27,28] The resonant wavelength and SPR intensity depend on the nature of the metal, the surrounding

environment, the size and the shape of the metallic nanostructures.[27] The main focus of the majority of these studies lies on shifting the activity window of a wide bandgap semiconductor like TiO_2 to the visible range of the spectrum.[29,30] Although this shift offers an innovative solution to the poor solar light response of TiO_2, there is still ample room for improvement, as established overall quantum efficiencies under visible light remain several orders of magnitude lower compared to those of traditional TiO_2-based UV photocatalysis.[29] In this work, the aim is not to enhance the solar light response but to use UV light to its full potential by working with silver nanoparticles that display SPR in the UV-region of the solar spectrum. To increase the light efficiency, convenient use can be made of the strong electric near-field enhancement which SPR entails. The build-up of these intense local electric fields allows an efficient concentration of the incident photon energy in small volumes near the nanostructures.[27] Since the rate of electron-hole pair formation is proportional to the intensity of the electric field, a drastic increase in charge carrier formation occurs. In order for this plasmonic "lens effect" to work, an energy match between the bandgap energy of the semiconductor, the spectral output of the light source and the energy associated with the SPR is crucial.[31] For TiO_2 under UVA irradiation, this criterion is met especially for silver nanoparticles, with an SPR band around 390 nm.[27,32] Silver nanoparticles without stabilization, however, are prone to oxidation and aggregation. Therefore, a core-shell structure consisting of a metallic core surrounded by a thin protective shell is applied to overcome these stability issues. The protective shell consists of polyelectrolytes which are wrapped around the nanoparticles based on the layer-by-layer protocol first described by Decher in 1997.[33] Recently, our research group has shown that the LBL technique is a highly controllable strategy for the preparation of core-shell silver nanoparticles with control over the thickness of the polymer shell up to the sub-nanometer level and effectively prevents oxidation of silver nanoparticles without compromising their plasmonic properties.[34]

It is shown that our (silver-modified) glass spiral reactor offers an attractive solution for photocatalytic air purification with high degradation efficiencies at much shorter gas residence times compared to conventional reactor geometries of the same dimensions and catalyst loading.

2 Experimental

2.1 Gas phase photoreactor design

2.1.1 Spiral reactor

The reactor consists of a 2620 mm long borosilicate glass tube (> 95% transmission) of 4 mm inner diameter, that is hand-blown into a spiral of 200 mm length and 48 mm width as outer dimensions. A Philips Cleo UVA lamp (25 W, λ_{max} 350 nm) is positioned longitudinally in the center as schematically depicted in Figure 1A, resulting in an incident intensity of 4.2 mW cm^{-2}, measured at a distance of 1.3 cm, corresponding to the distance between the lamp and the reactor, with a calibrated Avantes Avaspec-3648 irradiance spectrometer. A photograph of the spiral reactor used in this work is shown in Figure 1B.

2.1.2 Annular reactor

To benchmark the results of the spiral reactor, an annular reactor of the same outer dimensions as the spiral reactor was constructed. This annular reactor is schematically depicted in Figure 1C and consists of two concentric cylinders (borosilicate glass, > 95% transmission), one outer cylinder of 48 mm and an inner cylinder of 24 mm, both 200 mm long. Both ends were sealed with butyl rubbers sandwiched between a dedicated closing mechanism to ensure airtightness (Figure 1D). The same lamp as in 2.1.1 is positioned longitudinally in the center.

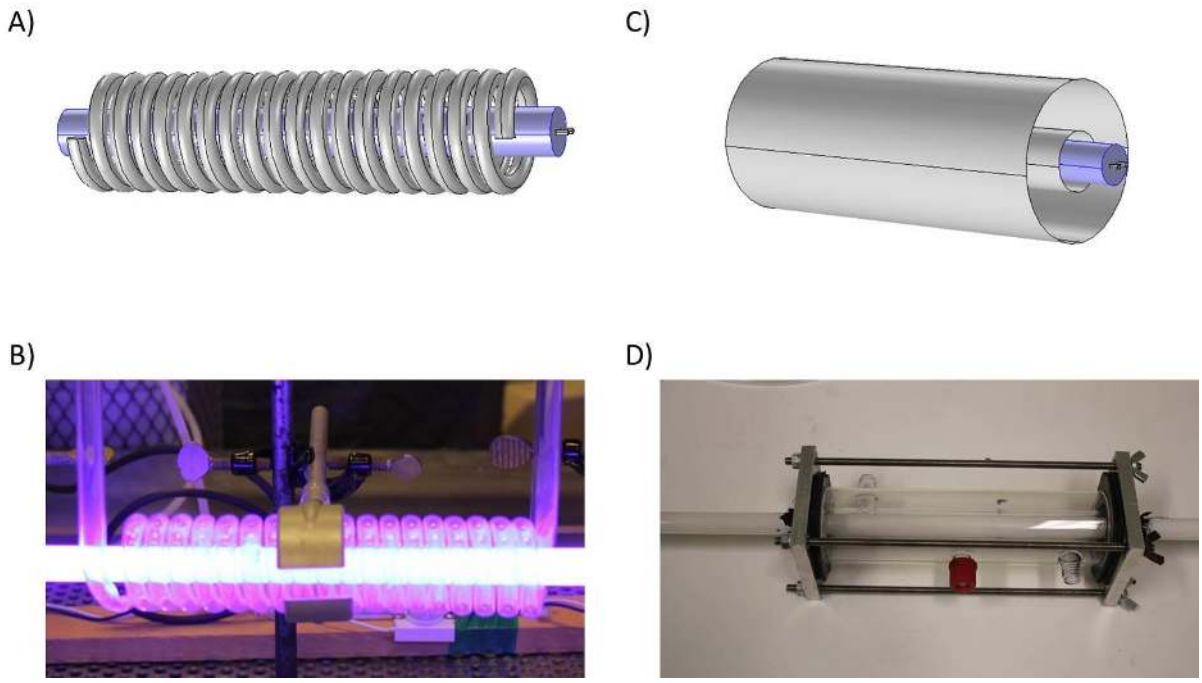

Figure 1. Gas phase photocatalytic reactor designs used in this work. A) schematic representation of the spiral reactor and B) photograph of the actual spiral reactor used in our study. C) schematic representation of an annular photocatalytic benchmark reactor and D) photograph of the latter as used in our study.

2.2 Synthesis of silver-polymer core-shell nanoparticles

The synthesis of silver nanoparticles was based on the procedure described by Bastús *et al*.[35] A 100 mL aqueous solution of sodium citrate (5 mM) and tannic acid (0.05 mM) was heated under vigorous stirring until boiling commenced. At this point, 1 mL of a 25 mM aqueous silver nitrate ($AgNO_3$) solution was added and left boiling for 30 min. Immediately after the addition of $AgNO_3$, the solution became bright yellow. To remove the excess of tannic acid and citrate, the batch was centrifuged at 12,000 g for 30 min and the resulting nanoparticles were redispersed in 25 mL Milli-Q-water (ρ = 18.2 MΩ).

To avoid oxidation and aggregation of silver nanoparticles, a core-shell structure of polymers based on the LBL method is applied, as reported recently by our group.[34] The silver core-shell particles were constructed using stock solutions of polyelectrolytes polyallylamine hydrochloride (PAH, Mwt 17.5 KDa, Sigma-Aldrich) and polyacrylic acid (PAA, MW 2 KDa, Sigma-Aldrich) prepared in Mili-Q-

water. Prior to use, the polymer solutions were sonicated for 30 min. For the deposition of the first polyelectrolyte layer, *i.e.* PAH, 25 mL of silver colloidal solution was added drop-wise to 13 mL of 5 g/L PAH in a glass vial under vigorous stirring, which continued for 20 min under dark conditions at room temperature. The resulting PAH capped silver nanoparticles were centrifuged (12,000 g) for 40 min in 1.5 mL Eppendorf tubes in order to remove the excess polyelectrolyte. The particles were redispersed in Milli-Q water as a washing step, centrifuged once more and finally the obtained colloids were again redispersed in 25 mL of Milli-Q-water. The deposition of the second layer was achieved using 10 g/L PAA using a similar approach as for the first layer, only the centrifugation speed was lowered (10,000 g) to avoid the formation of hard pellets. The procedure was repeated until silver nanoparticles were obtained with four polymer layers. A FEI Tecnai Transmission Electron Microscope (TEM) operated at 200 kV was used to visualize the core-shell structure of nanoparticles.

2.3 Catalyst coating procedure and photocatalytic tests

The photocatalytic degradation of air pollutants is studied under ambient conditions. Acetaldehyde is studied as a model compound. Firstly, the TiO_2 coating was introduced in the spiral photoreactor via an easy and affordable coating protocol, in which commercially available TiO_2 powder is simply suspended in ethanol.[6,22] An important design feature is the optimization of the catalyst loading in conjunction with the resulting light transparency of the coated surface. Rather than performing thickness measurements, our optimization method was purely based on light transmission. In order to establish the most ideal coating conditions, different glass slides were coated with three different suspensions of TiO_2 in ethanol (0.5, 1 and 2 wt%) by pouring 3 mL of the suspension over the glass slide in one smooth motion, dried at 25°C for 6 h and then the transmission of UV light passing through the glass slides was measured using a calibrated spectroradiometer (Avantes Avaspec). The coating procedure was repeated to introduce higher catalyst loadings. Using this approach the goal was to obtain a coating condition that results in 50% light transmission which is considered optimal since both in the spiral and annular reactors, emitted photons are assumed to cross two coating

layers before exiting the geometry. The results of the 'coating-transmission calibration' in Figure 2 show that one coating cycle using a 1 wt% suspension resulted in approximately 50% transmission, as required.

For coating the spiral reactor, 237 mg of TiO_2 P-25 (Evonik) was added to 30 mL of ethanol to obtain a 1 wt% suspension and stirred ultrasonically for 30 min. The suspension was poured in one smooth motion through the spiral reactor to obtain a thin semi-transparent white layer of TiO_2. It was verified that the appearance of the coating was indeed similar to what was obtained by coating a planar glass slide with the same 1 wt% suspension. To remove the solvent, a continuous air flow was sent through the reactor overnight in the presence of UV light (leading to photocatalytic degradation of adsorbed ethanol). When measuring the actual resulting transmission of UV light throughout the coated spiral, still nearly 30% transmission was recorded. It should be noted though this is a rather misleading value: the windings of the spiral are not completely tight (practical limitation experience by the glass blower, see Figure 1a and 1b), so part of the light is still escaping the geometry through gaps in between windings. This may represent the starting point for further optimization of the outer shape or dimension of this type of photo-reactor.

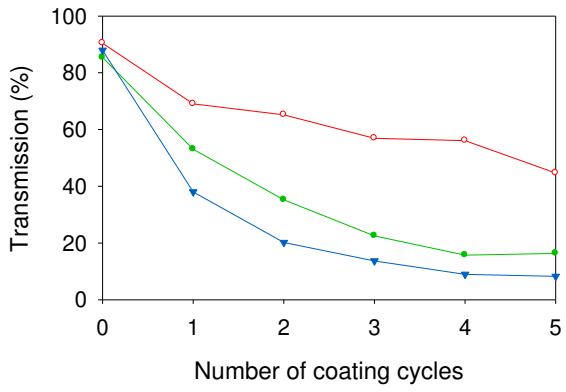

Figure 2. Transmission of different TiO_2 coatings on glass slides as a function of the number of coating cycles with different TiO_2 suspensions in ethanol: 0.5 wt% suspension (red ○), 1 wt% (green ●) and 2 wt% (blue ▼).

The procedure described above resulted in a catalyst coverage of 0.020 ± 0.001 mg cm^{-2} (corresponding to a total catalyst loading of 6.6 ± 0.4 mg in the entire reactor). The latter is determined by constructing a calibration curve that relates UV LED light transmission to well-known surface coverages of TiO_2 on glass, obtained by (repeated) drop casting of known amounts of a very well dispersed 0.05 wt% TiO_2 suspension in ethanol on cleaned cover slips (Figure 3).

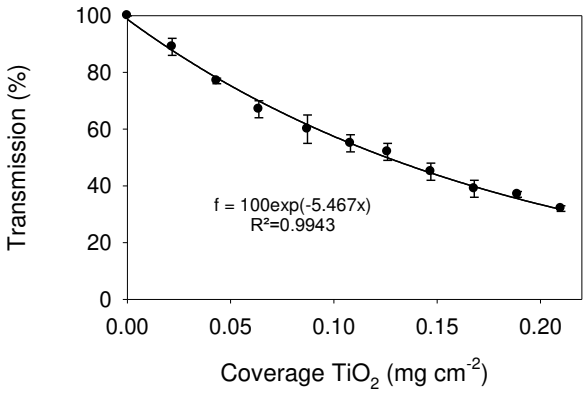

Figure 3. Calibration curve of transmission as a function of TiO_2 coverage (mg cm^{-2}).

Deposition of polymer-capped silver nanoparticles was achieved by simply pouring the as-obtained colloidal solution from 2.2 through the coated spiral reactor once. The reactor was dried overnight by flushing with air.

The reactor (Figure 1B) was mounted on a fully automated photocatalytic gas test setup of which the operation is amply explained in previous work.[36,37] In all tests, acetaldehyde was selected as target pollutant (Messer, 1% in N_2). The total flow rate was altered between 200 and 2000 mL min^{-1} to investigate the effect on the degradation efficiency. Depending on the experiment, the inlet concentration of acetaldehyde was set at 30 ppmv, 200 ppmv or 400 ppmv in dry air, as will be specified below. Prior to the photocatalytic degradation phase, adsorption-desorption equilibrium was established in dark conditions (30 minutes). Next, the lamp was turned on for 20 minutes. The degradation of acetaldehyde was determined as the steady state concentration of CO_2 produced under UV illumination, over twice the acetaldehyde inlet concentration (as two moles of CO_2 are

produced per mole of acetaldehyde). In between different experiments with the same reactor, the catalyst coating was regenerated by flushing with air for 1 h under illumination. Repetitive experiments showed no observable catalyst deactivation.

For the validation of the spiral photocatalytic reactor, the efficiency was compared with an annular reactor of the same outer dimensions and identical catalyst loading. Two different cases were considered for this annular reactor. In the first case, only the inner wall of the outer cylinder was coated with 30 mL of a 1.1 wt% suspension of TiO_2 in ethanol to result in the same total amount of TiO_2 as present in the spiral reactor (6.6 mg). In the second case, both the inner wall of the outer cylinder, as well as the outer wall of the inner cylinder were coated. In that case both cylinders were coated with a 0.73 wt% suspension of TiO_2 in 30 mL ethanol that again resulted in the same total amount of TiO_2 as in the spiral reactor (6.6 mg).

A residence time distribution (RTD) experiment was performed by injecting a ten second step of 40 mL of 1% ethylene in N_2 (Messer) as a tracer molecule in a total air flow rate of 1600 mL/min, which was sent through both reactor geometries. The concentration of ethylene in the outflow was monitored on-line and in real-time by FTIR spectroscopy. The resulting RTD thus reflects the distribution of ethylene in the entire setup including ducts, detection cell and reactor, but since only the latter is altered over different experiments, all changes in the RTD can be exclusively attributed to the reactor geometry alone.

3 Results and discussion

At first, our hypothesis of achieving an optimal catalyst coating by calibrating the resulting light transmission was verified. The idea was to aim for 50% transmission, since the light roughly has to cross two coated surfaces. As derived from Figure 2, a single coating step with a 1 wt% suspension of TiO_2 P25 in ethanol leads to this transmission target of 50%. This hypothesis was proven experimentally by coating the spiral reactor with increasing amounts of TiO_2 and measuring the

resulting photocatalytic degradation of 200 ppmv acetaldehyde at a total flow rate of 400 mL min^{-1}. The results in Figure 4 clearly illustrate that the degradation efficiency increases when increasing the suspension concentration up to 1 wt%, which can be explained by more effective use of incident photons by the increasing amount of catalyst present in the reactor. After reaching a maximum for the 1 wt% suspension, the degradation efficiency again drops for the 1.5 wt% suspension, which is attributed to an excessive amount of coating that blocks (scatters) part of the incident photon flux and prevent full photo-activation of the inner spiral surface in contact with the pollutants.

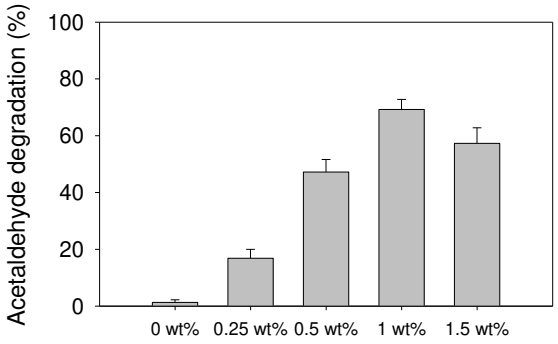

Figure 4. Photocatalytic degradation of acetaldehyde (200 ppmv in air at 400 mL min^{-1}) using the spiral reactor coated with different suspensions of TiO_2 in ethanol.

The photocatalytic activity of the two different reactor geometries (spiral *versus* annular) were compared towards the photocatalytic degradation of acetaldehyde. In these experiments, the concentration of acetaldehyde was kept constant at 30 ppmv while the total volumetric flow rate was altered between 200 mL min^{-1} and 2000 mL min^{-1}, which are the extrema of our setup. Since our aim was to compare reactor geometries of the same outer dimensions, both the spiral and the annular reactors were 200 mm long and 48 mm wide. Since the annular type reactor is composed of two cylinders, the most evident way to compare it with the spiral reactor is to coat both cylinders. The outer cylinder only coated from the inside and the inner cylinder only coated on the outside. This means, however, that although the amount of catalyst was kept the same, *i.e.* 6.6 mg, the total available surface was significantly larger for the annular reactor than for the spiral reactor (452 cm^2

and 329 cm² respectively). Alternatively, only the outer cylinder of the annular reactor was coated from the inside. This way, a total amount of 6.6 mg TiO_2 was coated on a surface of 302 cm² which is very close to the total available surface of the spiral reactor. All geometrical parameters are summarized in Table 1.

As can be derived from the results in Figure 5, the spiral reactor outperforms both the single coated cylinder and the double coated cylinder over the entire set of reaction conditions. Although the outer dimensions of the reactor are identical, the internal volumes are not. For the annular reactor, the volume is 271 cm³ whereas the reactor volume of the spiral is only 33 cm³ (Table 1). This means that the residence time of acetaldehyde in the spiral reactor is about 8 times shorter than for the annular reactor. In other words, the same amount of acetaldehyde is flowing through the spiral reactor 8 times as fast as through the annular reactor and still the degradation efficiency is significantly higher, especially at higher flow rates (*i.e.* shorter residence time). It can thus be concluded that the spiral reactor provides a very compact solution for the effective and fast degradation of VOC in a short period as compared to conventional photocatalytic reactor types. This outstanding performance is attributed to (1) homogeneous illumination over the entire reactor length (characteristic to concentric photoreactor design in general), (2) a coated layer optimized towards light transmission, and (3) intense (yet short) contact between gaseous reagents and the irradiated surface over the entire spiral length due to the narrow tube diameter. The latter can be explained due to the low Reynolds numbers in both reactors (i.e. < 15). This implies diffusion is the sole mechanism for transport of molecules to and from the surface, perpendicular to the direction of flow. It is evident this process proceeds more effectively for the narrow tube of the spiral reactor.

Table 1. Parameters of the different photocatalytic reactor designs

	Length (cm)	**Reactor volume (cm³)**	**Catalyst loading (mg)**	**Coated surface (cm²)**	**Coverage (mg/cm²)**
Spiral	20	33	6.6 ± 0.4	329	0.020 ± 0.001
Annular	20	271	6.6 ± 0.4	302[a]	0.022 ± 0.001
				452[b]	0.015 ± 0.001

[a]If only the outer cylinder is coated; [b]If both inner and outer cylinders are coated

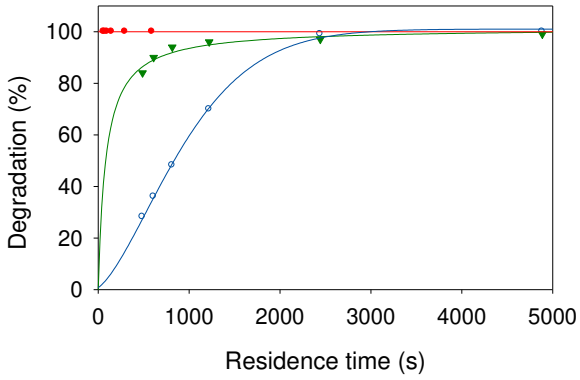

Figure 5. Photocatalytic degradation of acetaldehyde for different flow rates using different types of reactor geometries (30 ppmv in air, flow rates ranging from 200 to 2000 mL min^{-1}). Red ● indicate the spiral reactor, the green ▼ the double coated cylinder and the blue ○ the single coated cylinder.

Residence time distribution (RTD) functions for the spiral reactor and annular reactor are shown in Figure 6. The RTD function, E(t), is calculated as the FTIR absorbance of ethylene divided by the integrated absorbance over the entire time range (equal for both experiments: 5.57 ± 0.05). The first moment (average residence time) and second moment (degree of dispersion around the average residence time) were calculated as described by Levenspiel.[38] The former was equal for both reactors (20.3 ± 0.3 s), the latter differed slightly between the two reactors (spiral reactor: 54 s^2; annular reactor: 77 s^2). The later breakthrough of ethylene (onset of the RTD curve) observed for the spiral reactor compared to the annular reactor, might indicate some slightly longer dwelling of molecules in the spiral reactor, which could improve the interaction of gaseous pollutants with the coated reactor walls. It should be noted, however, that the difference in RTD functions is altogether quite small, and thus no significant difference in by-passing of gas can be claimed.

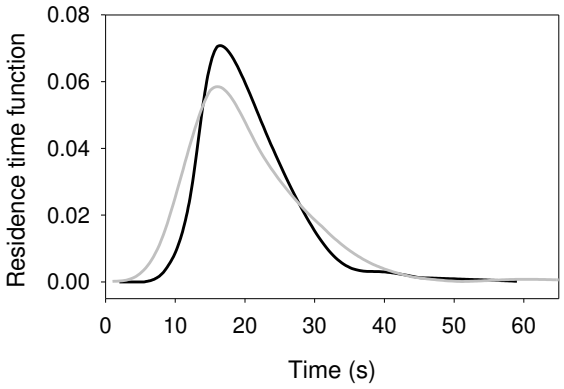

Figure 6. Comparison of the residence time function E(t) for the spiral reactor (black curve) and annular reactor (gray curve).

Finally, silver nanoparticles, stabilized by four polymer layers (Ag/(PAH/PAA)) were added to the TiO_2 coating in the spiral reactor. Figure 7 shows a TEM image in which a thin, uniform polymer shell is clearly visible. This image shows the degree of nanometer-level control on the thickness of the polymer shell that is offered by the LbL method. The total amount of silver loading on TiO_2 could not be determined accurately. In previous work on similar samples the loading was estimated to be well below 1 wt%.[34]

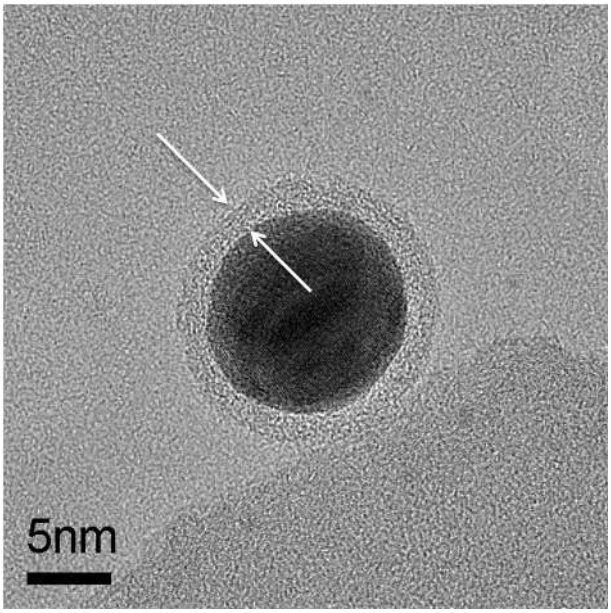

Figure 7. TEM image of silver core-shell nanoparticle with four polyelectrolyte layers (Ag/(PAH/PAA)).

The degradation of acetaldehyde was again used as a test to evaluate the difference between bare TiO_2 and silver-modified TiO_2. In these experiments a total flow rate of 200 mL min^{-1} was used with an acetaldehyde concentration of 400 ppmv. A drastic increase in the inlet concentration was required since for the 30 ppmv inlet concentration in the experiments above 100% acetaldehyde degradation was already achieved over the entire flow regime. The results depicted in Figure 8 show that under these conditions the TiO_2-coated spiral results in 50% acetaldehyde degradation. Upon addition of LbL-stabilized silver nanoparticles, an activity increase of 100% is obtained and complete removal of acetaldehyde is achieved. This is attributed to the enhanced electric near-field induced by SPR on these protected silver nanoparticles under UV illumination.[34] The core-shell silver nanoparticles show a plasmon band around 400 nm that overlaps with the TiO_2 P25 absorbance spectrum and the light source intensity spectrum. It is shown by Ingram *et al.* that this condition has to be fulfilled for optimal plasmonic near-field enhancement of the photocatalytic activity.[31] The particular usefulness, structure-activity relation and stability of the LbL-capped silver nanoparticles used in this final case study, are fully documented in our recent work by Asapu et al.[34]

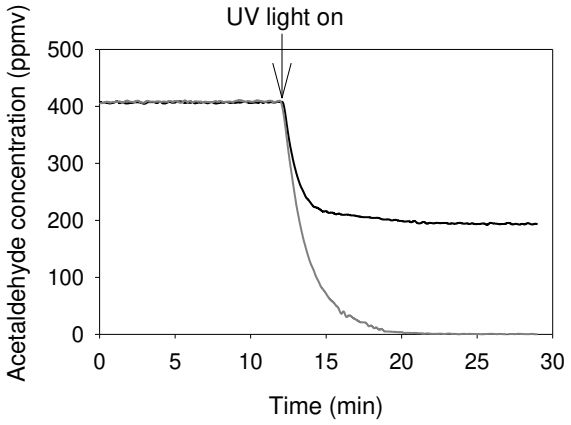

Figure 8. Degradation of Acetaldehyde with TiO_2 (black curve) and Ag@TiO_2 (gray curve). An increase of 100% in degradation efficiency is observed upon modification of TiO_2 with Ag core-shell nanoparticles. (Inlet conditions: 400 ppmv acetaldehyde at a total flow rate of 200 mL min^{-1})

To conclude, we end with an outlook on future possibilities offered by such a plasmon-enhanced spiral photoreactor design. The addition of gold or silver/gold alloy nanostructures would enable to not only harvest UV photons, but photons from the entire UV/Vis region of the solar spectrum, as we recently showcased by means of a 'rainbow' broadband plasmonic catalyst.[39] For the effective harvesting of solar photons we suggest a slight variation on the reactor geometry by translating a 3D spiral (helix) to a planar 2D spiral that can be oriented directly towards the sun. We will communicate our results on these advancements soon.

4 Conclusion

In this work, it is shown that an optimized spiral photocatalytic reactor outperforms a conventional annular photocatalytic reactor of the same outer dimensions and catalyst loading for the degradation of acetaldehyde as a model VOC. Particular attention has been paid to the optimization of the catalyst coating procedure by calibrating the resulting light transmission as a function of catalyst loading. The spiral reactor showed 100% degradation efficiency over a large range of flow rates whereas the annular reactor did not reach full degradation for gas residence times as high as 1000 s. Furthermore it is demonstrated that the addition of stabilized silver nanoparticles, encapsulated by a thin polymer shell, has a significant positive effect on the spiral's performance and resulted in doubling of the degradation efficiency for an acetaldehyde inlet concentration as high as 400 ppmv. With this we provide a powerful and compact reactor solution for fast and efficient VOC degradation.

5 Acknowledgements

N.B. wishes to thank the University of Antwerp for financial support. N.C. and S.B. acknowledge financial support from European Research Council (ERC Starting Grant #335078-COLOURATOM). S.W.V. acknowledges the Research Foundation – Flanders (FWO) for a postdoctoral fellowship.

6 References

[1] S.W. Verbruggen, TiO2 photocatalysis for the degradation of pollutants in gas phase: From morphological design to plasmonic enhancement, J. Photochem. Photobiol. C Photochem. Rev. 24 (2015) 64–82. doi:10.1016/j.jphotochemrev.2015.07.001.

[2] P.-A. Bourgeois, E. Puzenat, L. Peruchon, F. Simonet, D. Chevalier, E. Deflin, C. Brochier, C. Guillard, Characterization of a new photocatalytic textile for formaldehyde removal from indoor air, Appl. Catal. B Environ. 128 (2012) 171–178. doi:10.1016/j.apcatb.2012.03.033.

[3] M. Le Bechec, N. Costarramone, T. Pigot, S. Lacombe, Gas-Phase Photooxidation: Reactors and Materials, Chem. Eng. Technol. 39 (2016) 26–38. doi:10.1002/ceat.201500349.

[4] J. Mo, Y. Zhang, Q. Xu, J.J. Lamson, R. Zhao, Photocatalytic purification of volatile organic compounds in indoor air: A literature review, Atmos. Environ. 43 (2009) 2229–2246. doi:10.1016/j.atmosenv.2009.01.034.

[5] T.N. Obee, S.O. Hay, Effects of Moisture and Temperature on the Photooxidation of Ethylene on Titania, Environ. Sci. Technol. 31 (1997) 2034–2038. doi:10.1021/es960827m.

[6] V. Puddu, H. Choi, D.D. Dionysiou, G. Li Puma, TiO2 photocatalyst for indoor air remediation: Influence of crystallinity, crystal phase, and UV radiation intensity on trichloroethylene degradation, Appl. Catal. B Environ. 94 (2010) 211–218. doi:10.1016/j.apcatb.2009.08.003.

[7] I. Salvadó-Estivill, A. Brucato, G. Li Puma, Two-Dimensional Modeling of a Flat-Plate Photocatalytic Reactor for Oxidation of Indoor Air Pollutants, Ind. Eng. Chem. Res. 46 (2007) 7489–7496. doi:10.1021/ie070391r.

[8] S.W. Verbruggen, S. Lenaerts, S. Denys, Analytic versus CFD approach for kinetic modeling of gas phase photocatalysis, Chem. Eng. J. 262 (2015) 1–8. doi:10.1016/j.cej.2014.09.041.

[9] J. Mo, Y. Zhang, R. Yang, Novel insight into VOC removal performance of photocatalytic

oxidation reactors, Indoor Air. 15 (2005) 291–300. doi:10.1111/j.1600-0668.2005.00374.x.

[10] F. Jović, V. Kosar, V. Tomašić, Z. Gomzi, Non-ideal flow in an annular photocatalytic reactor, Chem. Eng. Res. Des. 90 (2012) 1297–1306. doi:10.1016/j.cherd.2011.12.014.

[11] V. Keller, P. Bernhardt, F. Garin, Photocatalytic oxidation of butyl acetate in vapor phase on TiO2, Pt/TiO2 and WO3/TiO2 catalysts, J. Catal. 215 (2003) 129–138. doi:10.1016/S0021-9517(03)00002-2.

[12] S.A. Larson, J.A. Widegren, J.L. Falconer, Transient Studies of 2-Propanol Photocatalytic Oxidation on Titania, J. Catal. 157 (1995) 611–625. doi:10.1006/jcat.1995.1326.

[13] U.R. Pillai, E. Sahle–Demessie, Selective Oxidation of Alcohols in Gas Phase Using Light-Activated Titanium Dioxide, J. Catal. 211 (2002) 434–444. doi:10.1006/jcat.2002.3771.

[14] C. Tang, V. Chen, The photocatalytic degradation of reactive black 5 using TiO2/UV in an annular photoreactor, Water Res. 38 (2004) 2775–2781. doi:10.1016/j.watres.2004.03.020.

[15] W.A. Jacoby, D.M. Blake, R.D. Noble, C.A. Koval, Kinetics of the Oxidation of Trichloroethylene in Air via Heterogeneous Photocatalysis, J. Catal. 157 (1995) 87–96. doi:10.1006/jcat.1995.1270.

[16] J. Peral, X. Domènech, D.F. Ollis, Heterogeneous photocatalysis for purification, decontamination and deodorization of air, J. Chem. Technol. Biotechnol. 70 (1997) 117–140. doi:10.1002/(SICI)1097-4660(199710)70:2<117::AID-JCTB746>3.0.CO;2-F.

[17] T. Van Gerven, G. Mul, J. Moulijn, A. Stankiewicz, A review of intensification of photocatalytic processes, Chem. Eng. Process. Process Intensif. 46 (2007) 781–789. doi:10.1016/j.cep.2007.05.012.

[18] W.K. Jo, G.T. Park, R.J. Tayade, Synergetic effect of adsorption on degradation of malachite green dye under blue LED irradiation using spiral-shaped photocatalytic reactor, J. Chem.

Technol. Biotechnol. 90 (2015) 2280–2289. doi:10.1002/jctb.4547.

[19] T.C. Machado, M.A. Lansarin, C.S. Ribeiro, Wastewater remediation using a spiral shaped reactor for photochemical reduction of hexavalent chromium., Photochem. Photobiol. Sci. (2014). doi:10.1039/c4pp00263f.

[20] Y. Wu, H. Yuan, X. Jiang, G. Wei, C. Li, W. Dong, Photocatalytic degradation of 4- tert -octylphenol in a spiral photoreactor system, J. Environ. Sci. 24 (2012) 1679–1685. doi:10.1016/S1001-0742(11)60995-9.

[21] N.M. Reis, G. Li Puma, A novel microfluidic approach for extremely fast and efficient photochemical transformations in fluoropolymer microcapillary films., Chem. Commun. (Camb). 51 (2015) 8414–7. doi:10.1039/c5cc01559f.

[22] S.W. Verbruggen, S. Ribbens, T. Tytgat, B. Hauchecorne, M. Smits, V. Meynen, P. Cool, J.A. Martens, S. Lenaerts, The benefit of glass bead supports for efficient gas phase photocatalysis: Case study of a commercial and a synthesised photocatalyst, Chem. Eng. J. 174 (2011) 318–325. doi:10.1016/j.cej.2011.09.038.

[23] J. Araña, A. Peña Alonso, J.M. Doña Rodríguez, J.A. Herrera Melián, O. González Díaz, J. Pérez Peña, Comparative study of MTBE photocatalytic degradation with TiO2 and Cu-TiO2, Appl. Catal. B Environ. 78 (2008) 355–363. doi:10.1016/j.apcatb.2007.09.023.

[24] J.H. Xu, F. Shiraishi, Photocatalytic decomposition of acetaldehyde in air over titanium dioxide, J. Chem. Technol. Biotechnol. 74 (1999) 1096–1100. doi:10.1002/(SICI)1097-4660(199911)74:11<1096::AID-JCTB145>3.0.CO;2-V.

[25] C.L. Bianchi, S. Gatto, C. Pirola, A. Naldoni, A. Di Michele, G. Cerrato, V. Crocellà, V. Capucci, Photocatalytic degradation of acetone, acetaldehyde and toluene in gas-phase: Comparison between nano and micro-sized TiO2, Appl. Catal. B Environ. 146 (2014) 123–130.

doi:10.1016/j.apcatb.2013.02.047.

[26] H.K. Seitz, F. Stickel, Acetaldehyde as an underestimated risk factor for cancer development: role of genetics in ethanol metabolism, Genes Nutr. 5 (2010) 121–128. doi:10.1007/s12263-009-0154-1.

[27] S. Linic, P. Christopher, D.B. Ingram, Plasmonic-metal nanostructures for efficient conversion of solar to chemical energy, Nat. Mater. 10 (2011) 911–921. doi:10.1038/nmat3151.

[28] E. Kowalska, O.O.P. Mahaney, R. Abe, B. Ohtani, Visible-light-induced photocatalysis through surface plasmon excitation of gold on titania surfaces, Phys. Chem. Chem. Phys. 12 (2010) 2344–2355. doi:10.1039/B917399D.

[29] W. Fan, M.K.H. Leung, J.C. Yu, W.K. Ho, Recent development of plasmonic resonance-based photocatalysis and photovoltaics for solar utilization, Molecules. 21 (2016). doi:10.3390/molecules21020180.

[30] P. Wang, B. Huang, Y. Dai, M.-H. Whangbo, Plasmonic photocatalysts: harvesting visible light with noble metal nanoparticles., Phys. Chem. Chem. Phys. 14 (2012) 9813–9825. doi:10.1039/c2cp40823f.

[31] D.B. Ingram, P. Christopher, J.L. Bauer, S. Linic, Predictive Model for the Design of Plasmonic Metal/Semiconductor Composite Photocatalysts, ACS Catal. 1 (2011) 1441–1447. doi:10.1021/cs200320h.

[32] H.A. Atwater, A. Polman, Plasmonics for improved photovoltaic devices, Nat Mater. 9 (2010) 205–213. 10.1038/nmat2629.

[33] G. Decher, Fuzzy Nanoassemblies: Toward Layered Polymeric Multicomposites, Science. 277 (1997) 1232–1237. doi:10.1126/science.277.5330.1232.

[34] R. Asapu, N. Claes, S. Bals, S. Denys, C. Detavernier, S. Lenaerts, S.W. Verbruggen, Silver-

polymer core-shell nanoparticles for ultrastable plasmon-enhanced photocatalysis, Appl. Catal. B Environ. 200 (2017) 31–38. doi:10.1016/j.apcatb.2016.06.062.

[35] N.G. Bastús, F. Merkoçi, J. Piella, V. Puntes, Synthesis of Highly Monodisperse Citrate-Stabilized Silver Nanoparticles of up to 200 nm: Kinetic Control and Catalytic Properties, Chem. Mater. 26 (2014) 2836–2846. doi:10.1021/cm500316k.

[36] T. Tytgat, B. Hauchecorne, M. Smits, S.W. Verbruggen, S. Lenaerts, Concept and validation of a fully automated photocatalytic test setup., J. Lab. Autom. 17 (2012) 134–43. doi:10.1177/2211068211424554.

[37] S.W. Verbruggen, S. Deng, M. Kurttepeli, D.J. Cott, P.M. Vereecken, S. Bals, J.A. Martens, C. Detavernier, S. Lenaerts, Photocatalytic acetaldehyde oxidation in air using spacious TiO2 films prepared by atomic layer deposition on supported carbonaceous sacrificial templates, Appl. Catal. B Environ. 160–161 (2014) 204–210. doi:10.1016/j.apcatb.2014.05.029.

[38] O. Levenspiel, Chemical reaction engineering, 3rd edition, John Wiley & Sons, 1999.

[39] S.W. Verbruggen, M. Keulemans, B. Goris, N. Blommaerts, S. Bals, J.A. Martens, S. Lenaerts, Plasmonic “rainbow” photocatalyst with broadband solar light response for environmental applications, Appl. Catal. B Environ. 188 (2016) 147–153. doi:10.1016/j.apcatb.2016.02.002.